


 Cite this: *RSC Adv.*, 2025, 15, 3427

Platinum(II) complexes of aryl guanidine-like derivatives as potential anticancer agents: between coordination and cyclometallation†

 Patrick O'Sullivan,^a Viola Previtali,^a Brendan Twamley,^a Celine J. Marmion,^b Aidan R. McDonald[✉] and Isabel Rozas^{✉*}

The preparation of a wide variety of Pt(II) complexes with aryl guanidines and their potential application as anticancer agents have been explored. A relatively facile synthesis of cyclometallated Pt(II) complexes of arylguanidines, preparation of Pt(II) guanidine coordination complexes and an *in situ* activation of platinum arylguanidine complexes with acetonitrile to create a bidentate aryl iminoguanidine Pt(II) complex were achieved. Cyclometallation methodology was extended to create a water-stable conjugate incorporating two Pt(II) ions and a diaryl bis-guanidine DNA minor groove binder. Several crystal structures were obtained confirming these complexation modes. The cyclometallated Pt(II) complexes were particularly stable to aqueous environments and were tested for Reactive Oxygen Species generation and anticancer activity in a leukaemia cancer cell line.

 Received 13th January 2025
 Accepted 20th January 2025

DOI: 10.1039/d5ra00310e

rsc.li/rsc-advances

Introduction

It is well known that platinum complexes like cis-platin and carboplatin play a crucial role in the treatment of several cancers. They exert their therapeutic activity by forming DNA adducts within cancer cells, thus inhibiting DNA replication and transcription and ultimately leading to cancer cell apoptosis or cell death.^{1,2} Platinum drugs are also widely employed in combination therapy regimens.^{3,4} Notwithstanding their success, platinum-based therapies also exhibit secondary adverse effects (myelosuppression, nephrotoxicity, ototoxicity, thrombocytopenia or extensive plasma protein binding) that limit their use and/or dose.⁵ The development of cancer drug resistance is also a major challenge. To overcome these unwanted shortcomings, new platinum-based derivatives are being continuously developed. These include but are not limited to non-classical Pt(II) complexes, polynuclear Pt(II) compounds, photoactivatable Pt(IV) complexes⁶ or multi-targeted Pt(II) and Pt(IV) complexes, as summarised in recent comprehensive reviews.⁷ The multi-targeted approach has led to highly efficacious Pt(II) complexes which not only target cancer cell DNA but also, amongst others, enzymes such as histone deacetylases, kinases, reductases, matrix metalloproteases and

DNA topoisomerases, peptides and intracellular proteins such as STAT3 and tubulin. Examples also include Pt-DNA targeting agents that carry vectors such as sugars and hormone or integrin receptors to enable them selectively target cancer cells.

Among the non-classical Pt-based derivatives, Pt(II) complexes of guanidine-like systems are particularly interesting. Guanidines have been shown to possess versatile biological properties with numerous reports of guanidine derivatives possessing anticancer, antibacterial, antifungal, antiprotozoal and antiviral activities and some guanidine-based drugs are already in clinical use, all of which are eloquently summarised by Roleira *et al.* in a 2023 comprehensive review.⁸ Guanidines are versatile ligands possessing a rich coordination chemistry. Different metal complexes with neutral guanidine, anionic guanidinate and dianionic guanidinate are known.^{9,10} For example, Jakupec and Keppler reported novel trans Pt complexes of guanidine synthesized by the nucleophilic addition of methylamine to di-alkyl cyanamide ligands of push-pull trans Pt nitrile complexes. Their *in vitro* assessment in different cancer cell lines indicated that the cytotoxicity of several *trans*-3,6 complexes was higher than that of *cis*-3,6 analogues. DNA interaction studies with some of these guanidine complexes confirmed that these compounds alter the DNA secondary structure, suggesting DNA as their possible target.¹⁰ Additionally, Carrillo-Hermosilla *et al.* published a very thorough review on the organometallic chemistry of guanidinate compounds, examining particular modes of coordination, reactivity and applications in catalysis or materials science.¹¹ Thirupathi *et al.* reported in 2013 a series of interesting *cis*, *trans* and cyclometallated guanidine Pt(II) complexes. They achieved complexation of symmetrically tri-substituted aromatic guanidines

^aSchool of Chemistry, Trinity College Dublin, 152-160 Pearse Street, Dublin 2, Ireland. E-mail: rozasi@tcd.ie; Tel: +353 1 896 3731

^bDepartment of Chemistry, RCSI University of Medicine and Health Sciences, 123 St. Stephen's Green, Dublin 2, Ireland

† Electronic supplementary information (ESI) available. CCDC 2391910–2391917. For ESI and crystallographic data in CIF or other electronic format see DOI: <https://doi.org/10.1039/d5ra00310e>



using *cis*-[Cl₂Pt(S(O)Me₂)₂] and NaOAc in refluxing methanol. Depending on the reflux time and nature of the substituents in the aryl systems, they achieved guanidine complexation or cycloplatination.¹² Furthermore, Nieto *et al.* reported the reaction of a Pt(II) reagent with ferrocene derivatives of substituted guanidines that produced the corresponding heterometallic complexes; further they proved that guanidine-based ferrocene–Pt complexes were active against different human cancer cells.¹³

Given the known propensity of the guanidium cation to form non-covalent interactions with the phosphate residues of DNA's minor groove helix and the fact that clinically used Pt(II) drugs also target DNA albeit at a different site, namely by Pt binding to DNA nucleobases, we sought to explore the chemistry and biological activity of novel guanidine Pt(II) complexes as a new class of anticancer agent. We had previously studied their suitability from a theoretical point of view,¹⁴ and found that the most favourable Pt(II) complexes with guanidine derivatives were monodentate coordinated systems. Informed by these theoretical studies, our goal was to develop Pt(II) complexes of aryl guanidine-like systems with the final aim to produce cytotoxic agents.

Results and discussion

Preparation of guanidine-like ligands

To explore the best Pt complexation approach, mono-guanidine aryl systems (phenyl, pyridine, benzyl) with different substituents (*p*-OMe, *o*-NH₂) were selected, not only to probe the electron density effect on the aryl ring, but also to obtain a diverse range of possible metal-binding domains, (*e.g.* pyridine N or *o*-NH₂ vs. guanidine/2-aminoimidazoline N atoms). Since complexation of guanidines with Pt may be carried out by direct reaction of the corresponding ligands with a Pt source, the corresponding aryl guanidine-based ligands were first synthesised (see details in ESI†). Thus, aryl guanidinium salts (1–5), 2-(iminophenyl)imidazolidinium (6) and benzylguanidinium (7) were prepared following standard methods (Fig. 1).

To prepare the corresponding Pt complexes, the conditions reported by Aitken *et al.*¹⁵ for the aminoguanidine complexation were followed by treating guanidinium salts 1 and 2 (5 eq.) with K₂PtCl₄ (1 eq.) in water in the absence of base. Precipitates, that were only soluble in DMSO, instantly formed corresponding to the tetrachloroplatinate salts of 1 and 2, clearly indicating that the use of the free base of these arylguanidinium salts was

required in order to achieve Pt complexation. Accordingly, different bases (NH₄OH, KO^tBu, KOH) in solutions of dichloromethane/water were explored to isolate the free base of 1 used as a model (Table 1). In all cases, the yields obtained were not ideal (0–66%, entries 1–3, Table 1) because the neutral guanidine was soluble in water. Considering that Yamada *et al.* had described the formation of a guanidine derivative in ethanol using sodium ethoxide as a base,¹⁶ and after adapting the procedure, the free base 8 was quantitatively obtained (entries 4–5, Table 1).

With these optimal conditions in hand (*i.e.*, 1.1 equiv. of sodium ethoxide in ethanol), conversion of the corresponding aryl guanidinium (1–5), 2-aminoimidazolinium (6) and benzyl guanidinium (7) salts to the corresponding free bases 8–14, was achieved with quantitative yields (Scheme 1).

Thus, seven guanidine-like ligands were prepared with the aim of forming the corresponding Pt(II) complexes.

Preparation of cyclometallated Pt(II) guanidine complexes

Once these mono-guanidines were prepared, different approaches for their complexation with Pt(II) were explored. First, commercial K₂PtCl₄ was reacted with phenylguanidine 8 in the presence of aqueous KOH at pH = 9 and pH = 13, at room temperature and at reflux, yielding in all cases a black precipitate of Pt(0) as the major product. Similarly, reaction of the free bases 8, 9 and 13 with K₂PtCl₄ in MeOH or H₂O at room

Table 1 Conditions screened for the generation of the free base of compound 1

Entry	Base	Solvent	Yield ^a
1	NH ₄ OH (5 eq.)	CH ₂ Cl ₂ /H ₂ O	0%
2	KO ^t Bu (5 eq.)	CH ₂ Cl ₂ /H ₂ O	66%
3	KOH (pH 13)	CH ₂ Cl ₂ /H ₂ O	41%
4	NaOEt (1.0 eq.)	EtOH	92% ^b
5	NaOEt (1.1 eq.)	EtOH	100%

^a Isolated yields. ^b Mixture of 8 and 1 (8%) as per ¹H NMR.

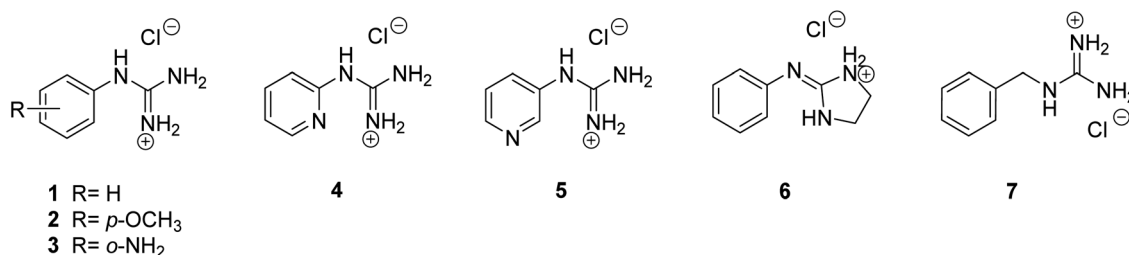
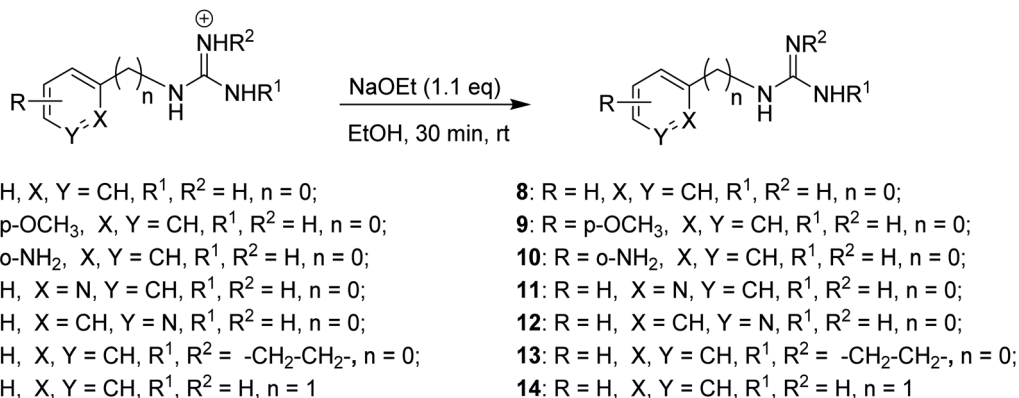


Fig. 1 Structures of the guanidinium-like hydrochlorides 1–7, prepared as models to explore the conditions for the preparation of guanidine–Pt(II) complexes.



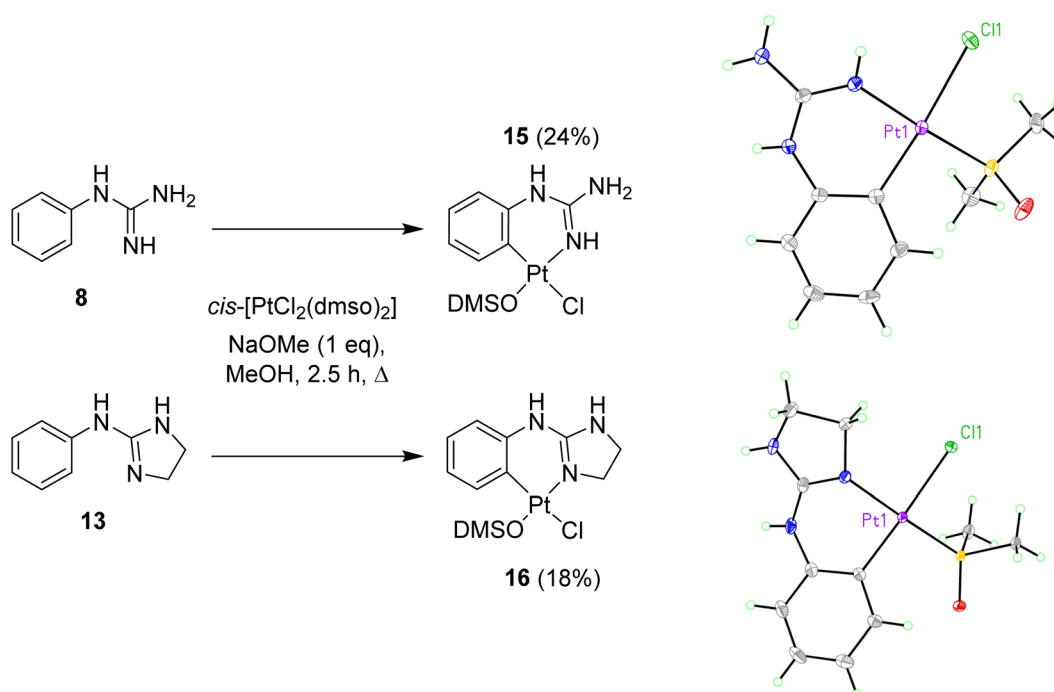


Scheme 1 Aryl guanidinium/2-aminoimidazolium derivatives converted to the corresponding aryl guanidine free base.

temperature in subdued lighting conditions led to decomposition to Pt(0). Next, considering that *cis*-[PtCl₂(DMSO)₂] had been reported to form Pt(II) complexes with guanidine N atoms,^{13,17,18} this agent was tested to achieve complexation of the aryl guanidines prepared.

Complex *cis*-[PtCl₂(DMSO)₂] was prepared as previously described in the literature.¹⁹ Initial attempts of complexation using two equivalents of **8** and *cis*-[PtCl₂(DMSO)₂] in THF or chloroform at reflux resulted in the recovery of starting materials. When the reaction was carried out with one equivalent of **8** in methanol at reflux, two products were obtained, the cationic precursor of the starting material (*i.e.* compound **1**) and a new derivative **15**. After filtration and solvent removal *in vacuo*, the product was dissolved in the minimum amount of DMSO and

precipitated out by addition of water. The solid obtained was characterised by NMR and IR spectroscopy. TOCSY and NOESY experiments, together with high temperature ¹H NMR experiments of **15**, showed Pt-complexation as indicated by satellite peaks at 6.3 ppm (NH) and 8.0 ppm (CH) (Fig. S1†). Additionally, the ¹³C NMR spectrum indicated coordination with DMSO and the IR spectrum showed an S–O stretch at 1091 cm⁻¹. Furthermore, low resolution mass spectrometry revealed an [M + H]⁺ peak at 443.02, with a characteristic isotope splitting pattern for Pt and matching a calculated formula of [C₉H₁₅ClN₃O₂S]⁺, thus suggesting that the fourth ligand must be Cl. Although there was no direct evidence of the arrangement of the Cl and DMSO ligands relative to the aryl guanidine, it was reasoned that DMSO would not bind *trans* due to the strong *trans*-effect of the cyclometallated

Scheme 2 Preparation of cyclometallated Pt(II) complexes **15** and **16** and crystal structures of the asymmetric unit in the corresponding complexes. Displacement ellipsoids are at 50% probability.

group. Taking all this data into account a structure for the cyclometallated compound **15** was proposed (see Scheme 2). As mentioned, the reaction of one equivalent of free base **8** with excess of *cis*-[PtCl₂(DMSO)₂] produced cyclometallated product **15** and guanidinium salt **1**. However, since a second equivalent of free **8** could act as a base and then generate a new molecule of free base **8** from the *in situ* formed salt **1**, an equivalent of NaOMe was added to optimise the synthetic procedure, yielding exclusively the cyclometallated derivative **15** (Scheme 2). The reaction mixture was purified by repeated precipitation from a concentrated DMSO mixture with water and crystals of suitable quality for X-ray crystallography were grown in darkness at room temperature over a period of three months by slow evaporation of water into a concentrated DMSO solution of **15**. Gratifyingly, the structure confirmed our solution phase assignment (see Scheme 2, Table S1 and details in ESI†).

Complex **15** crystallised in an orthorhombic unit cell (0.71 Å resolution); the relative configuration of the ligands was confirmed to be SP-4-4 (square planar 4-coordinate with the highest priority ligand, in this case Cl, *trans* to the fourth priority ligand, C). The strong *trans*-effect of C was demonstrated by the long Pt–Cl bond (2.4095(6) Å). The distances around the central guanidine C atom (C8) indicate that the double bond is localised between N10–C8 (1.306(3) Å) and that the other C–N bonds are single bonds in nature (*i.e.* N7–C8, 1.354(3) Å; and N9–C8, 1.350(3) Å). The N–Pt–C and Cl–Pt–S angles around Pt were 89.13(10)° and 92.57(2)° respectively, close to the ideal bond angle of 90° for a square planar complex. The crystal is stabilised by intermolecular hydrogen bonds (HBs) between the DMSO's O atom of one molecule and a H atom on the guanidine NH₂ of another molecule.

A similar reaction using 2-aminoimidazolidine **13** produced the corresponding cyclometallated complex **16** (Scheme 2, Table S1 and details in ESI†) and, under identical conditions for crystallisation as those used with **15**, suitable crystals for X-ray crystallography were formed and resolved (see Scheme 2). The crystal structure of **16** was very similar to that of **15**; the Pt–Cl bond length was 2.4117(4) Å, and the N–Pt–C and Cl–Pt–S angles

were 86.81(6)° and 87.785(15)°, and the unit cell was orthorhombic (0.71 Å resolution), in the space group *Pbca*. Like in complex **15**, the distances around the central guanidine C atom (C8) indicate a localised double bond between N9–C8 (1.312(2) Å) while N7–C8 (1.345(2) Å), and N12–C8 (1.365(2) Å) seem to be single bonds. The main difference in the crystal packing was that **16** contained an intermolecular HB between the DMSO's O¹ atom and the aniline-type N⁷H of another molecule.

When reactions of *cis*-[PtCl₂(DMSO)₂] with *p*-methoxy phenylguanidine **9**, pyridine guanidines **11** and **12**, and benzylguanidine **14**, were attempted in similar conditions, no products were obtained. However, the reaction with the *o*-amino phenylguanidine **10** yielded a bimetallic species (**17**, Fig. 2) In this complex, a combination of cyclometallated and non-cyclometallated interactions with each Pt(II) centre is observed. Small purple crystals of suitable quality for X-ray diffraction were grown from a mixture of DMSO and H₂O over a period of six weeks. Complex **17** crystallised in a monoclinic unit cell (*P2₁/n* space group, 0.80 Å resolution, Fig. 2, Table S1 and details in ESI†). One of the Pt–Cl bonds is long, (2.421(3) Å) whereas the other is shorter (2.329(3) Å), again showing the strong *trans*-effect of C, with N–Pt–C and Cl–Pt–S angles of 85.4(4)° and 93.38(11)° respectively. Contrary to what was observed in complexes **15** and **16**, distances around the central guanidine C atom (C8) point toward a delocalised double bond between N1–C7 (1.338(15) Å) and N3–C7 (1.313(14) Å), but this delocalization does not extend to N4–C7 (1.395(14) Å). When **17** was put in a solution of DMSO-*d*₆ at room temperature, the compound degraded and was insoluble in any other solvent.

Once suitable conditions were found for the preparation of some phenyl guanidine-like Pt(II) cyclometallated complexes we proceed to explore the requirements to prepare non-cyclometallated complexes.

Preparation of coordinated Pt(II) guanidine complexes

Aiming to prepare non-cyclometallated Pt(II) arylguanidine complexes, other Pt precursors were investigated. Thus, as in

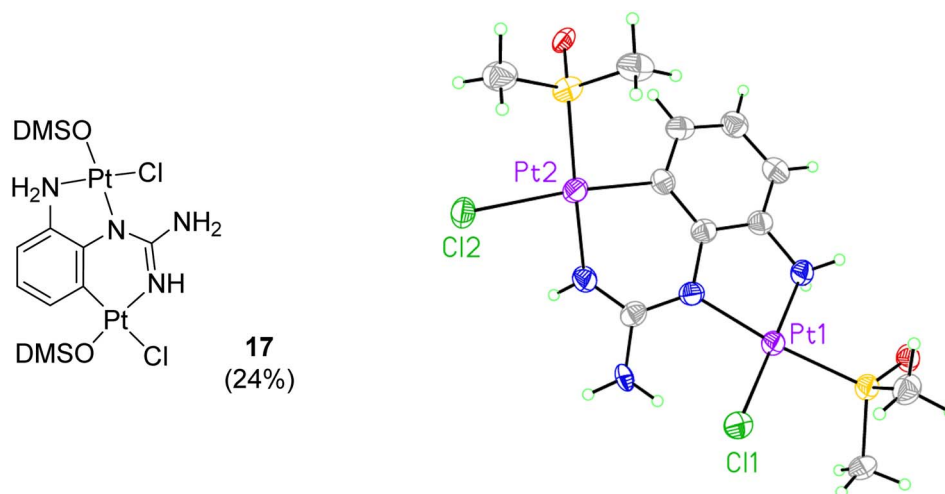
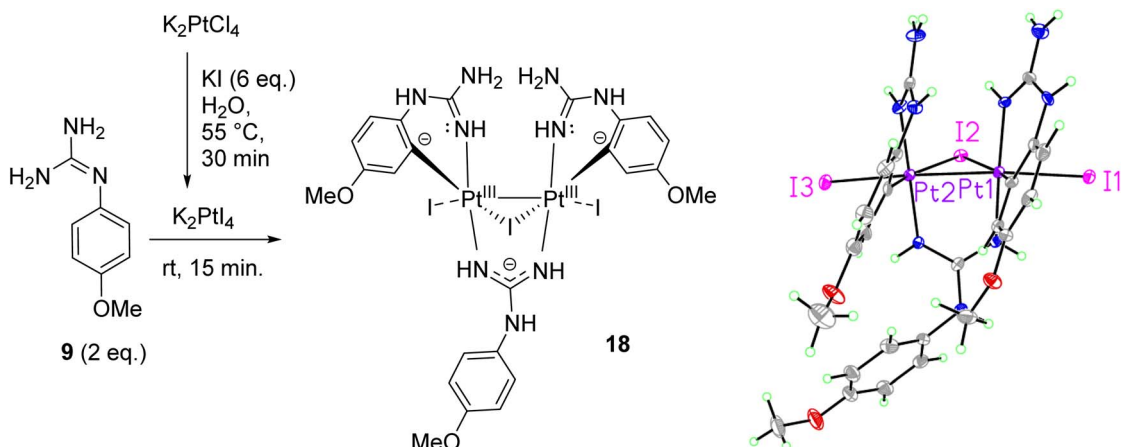


Fig. 2 Crystal structure of bimetallic complex **17**. Displacement ellipsoids are at 50% probability.



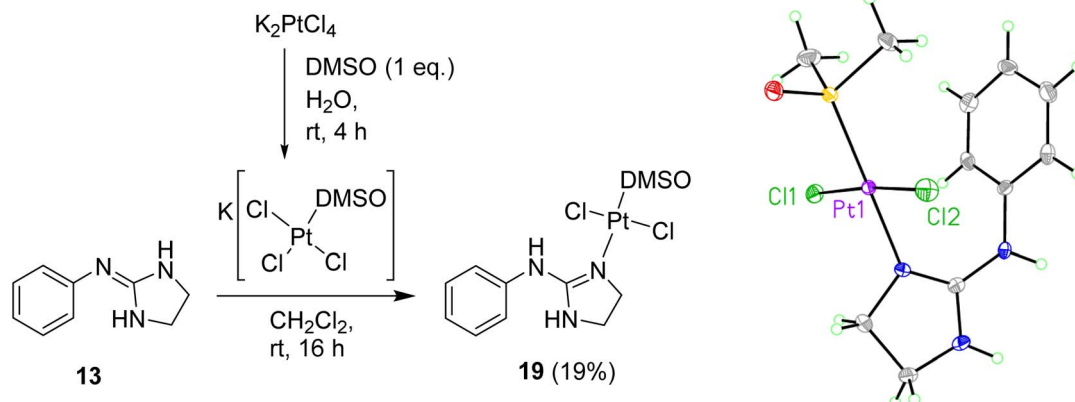


Scheme 3 Preparation of dinuclear Pt(III) complex **18** and crystal structure of the asymmetric unit. Displacement ellipsoids are at 50% probability.

the synthesis of cis-platin, K_2PtI_4 was tested with the electron-rich *p*-methoxyphenyl guanidine **9**. Accordingly, KI (6 eq.) was added to a solution of K_2PtCl_4 in H_2O at 55 °C for 30 min to generate K_2PtI_4 *in situ*.²⁰ Then, free base **9** (2 eq.) was added at room temperature and the reaction stirred for 15 min. A brown precipitate was isolated by filtration and washed with water, dissolved subsequently in hot EtOAc, purified by slow diffusion of Et_2O and then filtered. Crystals suitable for X-ray diffraction were grown from a standing solution of the filtrate to give **18** (Scheme 3, Table S1 and details in ESI[†]). The crystal structure of **18** ($P2_1/c$, monoclinic, 0.78 Å resolution) was not the expected coordination complex and contained a mixture of cyclometallated and non-cyclometallated guanidine Pt interactions. This structure was notable for many features (see Scheme 3). First, the dinuclear structure [$Pt_2(p\text{-OMe-PhGua})_3I_3$] contained a Pt–Pt bond (2.6149(3) Å), with each Pt bound to one axial I atom (Pt–I = 2.7690(4) Å and 2.7412(4) Å) and one bridging I atom (Pt–I = 2.7967(4) Å and 2.8230(4) Å, Pt–I–Pt = 55.459(9)°). Moreover, each Pt atom was forming a cyclometallated complex with two different molecules of **9** (C–Pt–N = 91.97(19)° and 87.41(19)°), and there was also a bridging guanidinate group of a third **9** molecule (each Pt–N bond = 2.021(4), 2.024(4) Å).

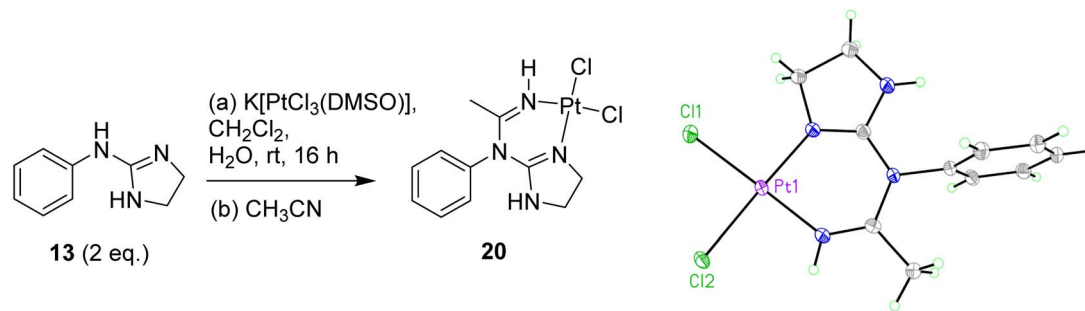
There are two solvent pores in the crystal (Et_2O and H_2O). The three negatively charged guanidine and iodine ligands require a +6 overall charge; hence, considering the almost symmetrical nature of the complex, we can assume these two Pt centres to be Pt(III). Most Pt(III) complexes are bimetallic, stabilising the unpaired radicals in a Pt–Pt bond; besides, reported bimetallic Pt(III) complexes have a distorted octahedral geometry, similar to that of **18**.^{21–23} The 1H NMR in $DMSO-d_6$ of **18** suggested that in solution the complex either decomposes or exists as a mixture of species.

To prevent cyclometallation, milder conditions based on work by Kukushkin were attempted.^{24,25} Thus, $K[PtCl_3(DMSO)]$ was synthesised *in situ*, followed by addition of water-soluble ligand **13** and CH_2Cl_2 at room temperature to obtain *trans*-dichloro coordination/non-cyclometallated complex **19** after evaporation of the organic layer at room temperature and quick chromatography on silica (Scheme 4). Since pure **19** decomposed in DMSO, all 1H NMR experiments were carried out in $DMF-d_7$ in which the complex is stable for at least seven days. The NOE experiments of compound **19** in $DMF-d_7$ showed that no such effect existed between the DMSO protons and any other protons on the molecule, suggesting that DMSO is *trans* to the 2-



Scheme 4 Preparation of Pt complex **19** and crystal structure of the asymmetric unit. Displacement ellipsoids are at 50% probability.





Scheme 5 Preparation of Pt complex **20** with the insertion of an acetonitrile molecule and crystal structure of the asymmetric unit. Displacement ellipsoids are at 50% probability.

aminoimidazoline ligand. High resolution mass spectrometry (ESI⁻) confirmed a molecular mass in agreement with the molecular formula C₁₁H₁₇Cl₂N₃OPtS. Crystals suitable for X-ray crystallography were grown over 12 h by slow diffusion of Et₂O into a concentrated solution of **19** in CH₂Cl₂ (see Scheme 4, Table S1 and details in ESI[†]). The crystal structure of complex **19** again demonstrated that DMSO binds to Pt *trans* to the guanidine-like N. The compound crystallised in an orthorhombic unit cell (resolution = 0.71 Å) and *P2*₁ *2*₁ *2*₁ space group. The crystal packing is stabilised by an intermolecular HB between the DMSO O¹ of one molecule and the aniline-type N⁶H of another molecule. The Pt–Cl bond lengths are both 2.3101(10) and 2.3130(10) Å and the Cl–Pt–Cl angle is 174.65(4)° whereas the N–Pt–S angle is 179.19(10)°.

Exploring other conditions for the obtention of **19** in better yields, two equivalents of free base **13** were reacted with K [PtCl₃(DMSO)] (Scheme 5), and when the crude reaction mixture from the organic layer was evaporated and re-dissolved in acetonitrile, crystals suitable for X-ray crystallography were isolated showing that, surprisingly, a reaction with a molecule of acetonitrile had taken place forming complex **20** (see Scheme 5, Table S1 and details in ESI[†]), which incorporates a methyl-imine into the structure.

The crystal structure of **20** is in a monoclinic unit cell (0.66 Å resolution), with space group *P2*₁/*c*. The Pt–Cl and Pt–N bond lengths are 2.3104(5), 2.3105(5) Å and 1.9749(17), 1.9794(17) Å, and the N–Pt–N and Cl–Pt–Cl angles are 88.36(7)° and 88.959(18)°, respectively. The three C–N bond lengths around the guanidine C atom are 1.303(3) Å (N1–C5), 1.352(3) Å (N4–C5), 1.385(3) Å (C5–N6), and the C–N bond lengths around the amidine C atom are 1.385(3) Å (N6–C7) and 1.284(3) Å (C7–N8). Clearly, the C–N bonds coordinated to Pt are the shortest, implying that the guanidine/amidine double bonds are more localised on these atoms (the CN triple bond in the acetonitrile solvate is much shorter, 1.13 Å). The other three C–N bonds to the guanidine or amidine C atom are intermediate in length between single and double bonds, demonstrating some degree of resonance. The C–N bonds to the imidazole CH₂ groups (1.453(3) Å and 1.476(3) Å) and to the aryl ring (1.452(2) Å) are clearly single bonds.

Regarding the possible mechanisms for the acetonitrile insertion, it is not clear whether the acetonitrile first coordinates to K[PtCl₃(DMSO)] and then undergoes nucleophilic

addition to coordinated 2-aminoimidazoline, if the coordinated acetonitrile is attacked by free 2-aminoimidazoline or if coordination of both ligands first takes place followed by C–N bond formation. Attack of coordinated 2-aminoimidazoline on uncoordinated acetonitrile was ruled out for steric reasons and the lack of precedence in the literature for nucleophilic attack on inactivated nitriles. In contrast, the strongly electrophilic properties of metal-acetonitrile complexes have been comprehensively reviewed.²⁶

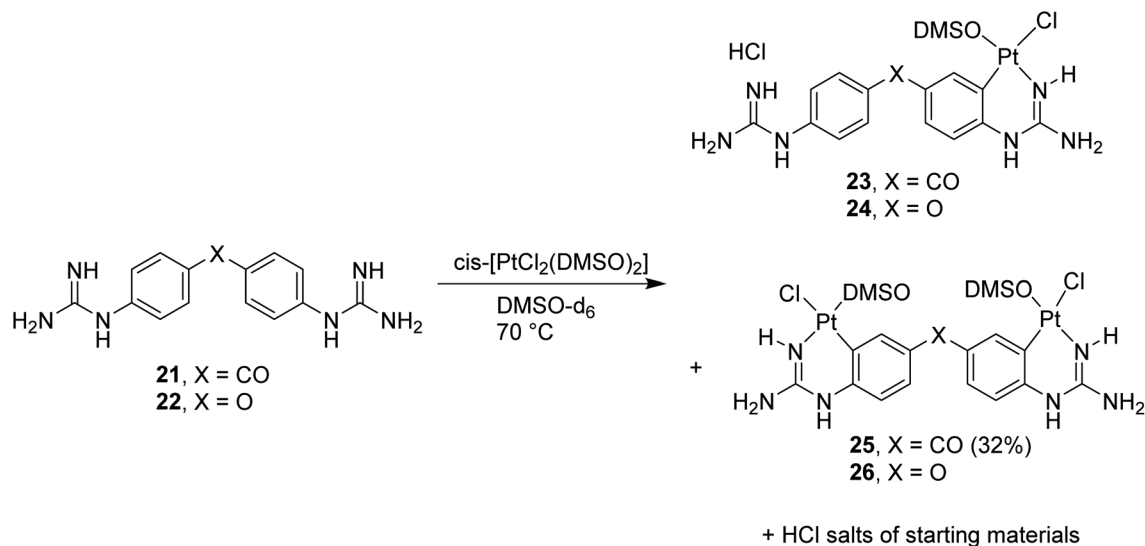
Further attempts to prepare more non-cyclometallated complexes like **19** with the rest of the free bases were unsuccessful as these compounds did not dissolve in the biphasic H₂O/CH₂Cl₂ solvent system at room temperature as used in Scheme 4. Thus, a single solvent system was attempted using either MeOH or THF with isolated K[PtCl₃(DMSO)]; however, these reactions gave a mixture of many compounds as adjudged by ¹H NMR.

Considering the results obtained so far, the cyclometallation of in-house diaryl bis-guanidine systems known to be good DNA minor groove binders was next attempted.

Preparation of cyclometallated complexes of bis-guanidine diaryl systems

Once the conditions for Pt cyclometallation of mono-guanidine-like systems **8** and **13** were established, the corresponding complexation of two bis-guanidinium systems, previously prepared in our lab showing good binding to the minor groove of DNA, was attempted. Thus, the free bases **21** and **22** were prepared and exposed to the corresponding cyclometallation conditions (*i.e.* *cis*-[PtCl₂(DMSO)₂], NaOCH₃, CH₃OH, 70 °C, 2 h; Scheme 6); however, only an insoluble yellow precipitate was formed in both cases instead of cyclometallation. Free bases **21** and **22** have two N atoms capable of forming bis-Pt complexes by coordinating with one N atom of another ligand and, hence, these potential oligomers could keep polymerising yielding the precipitate observed. To stop this hypothesised polymerisation and to identify the monomer complex, NaOCH₃ was removed, the solvent changed to DMSO-*d*₆, and the reaction with **21** was followed by ¹H NMR as indicated in the spectra shown in Fig. S2[†] confirming the formation of a mixture of the hydrochloride salt of the starting material, mono- and di-cyclometallation product.





Scheme 6 Cyclometallation reactions with bis-guanidine diaryl systems **21** (X = CO) and **22** (X = O) followed by ^1H NMR.

Thus, in the absence of MeOH or NaOCH₃ both reactions yielded the mentioned mixture as detected by NMR; however, isolation of the complexes proved difficult since all three species for each reaction were water soluble except for compound **25** (Scheme 6). Repeated dissolution of the crude mixture in DMSO, followed by precipitation with H₂O and filtration gave a filtrate from which carbonyl-linked **25** crystallised. Despite repeated attempts, purification of **23**, **24** or **26** did not yield adequate material for characterisation.

The X-ray structure of **25** (Fig. 3a, Table S1 and details in ESI†) was in agreement with the solution structure. The binuclear complex crystallised in an orthorhombic unit cell (0.80 Å resolution, *Pna2*₁ space group). Restraints and constraints were used to model the disorder in one of the Pt–Cl positions (72%/28% occupancy). There are three and a half water molecules per asymmetric unit.

Aiming to improve the preparation of cyclometallated Pt complexes of bis-guanidines **21** and **22**, many variations of the biphasic reaction from Scheme 5 were attempted, but no product

could be isolated. Switching to a mono-phasic system using MeOH with K[PtCl₃(DMSO)] and free base **21**, yielded again cyclometallated **25** after crystallisation from aqueous solution and a new sample suitable for X-ray diffraction was solved (Fig. 3b, Table S1 and details in ESI†). In this case, **25** crystallised in a triclinic unit cell (*P* $\bar{1}$ space group, 0.78 Å resolution) with two water molecules per complex. The Pt–N bonds were 1.995(4) and 2.008(4) Å. The Pt atoms were both square planar. Within the platinacycles, the C–Pt–N angles were both 89° (89.12(18) and 88.79(17)°). However, the C–Pt–S angle was 98° (98.44(14) and 97.91(13)°) in both cases. The overall molecule showed a helical twist. The Pt–Pt distance was *ca.* 6.09 Å and the angle between the planes of the square planar Pt geometries was 37.3(1)°. The dihedral angle between the planes of each benzene ring was 49.3(2)°.

In summary, bis-guanidine diaryl systems are likely to cyclometallate, even at room temperature and, therefore, non-cyclometallated Pt-complexes bound *via* a guanidine, even if isolated from a reaction mixture, would likely decompose under biological conditions.

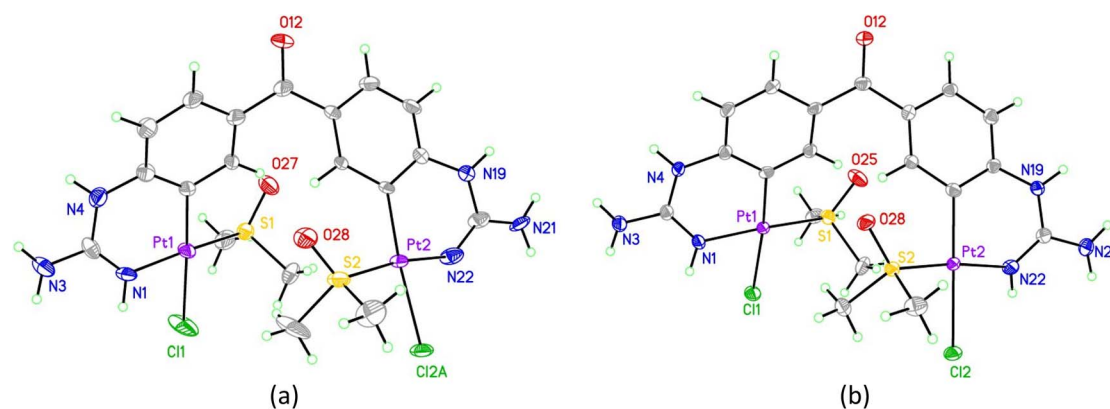


Fig. 3 (a) Asymmetric unit of the first crystal structure obtained of **25** showing the majority occupied disordered moiety (Pt2, Cl2A). (b) asymmetric unit of the second crystal structure obtained of **25**. In all structures displacement ellipsoids are at 50% probability. See ESI† for structures including solvents/disorder.



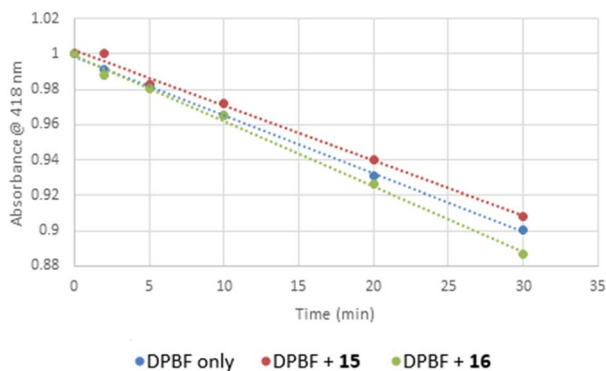


Fig. 4 Graph of change in DPBF absorbance vs. time in the presence of DMSO (blue dots, slope = -0.0033 min^{-1}), with **15** (red dots, slope = -0.0031 min^{-1}) and with **16** (green dots, slope = -0.0037 min^{-1}). All linear fits ($R^2 = 0.999$). Each data point is an average of two runs.

Assessment of cytotoxic potential of the cyclometallated complexes

Reactive oxygen species generation. Considering that Pt-cyclometallated complexes have been shown to generate singlet oxygen ($^1\text{O}_2$),²⁷ the potential Reactive Oxygen Species (ROS) generation for complexes **15** and **16** was investigated as a potential cytotoxic effect. The strongly absorbing compound 1,3-diphenyl-2-benzofuran (DPBF, $\lambda_{\text{max}} = 418 \text{ nm}$ in DMSO) is known to react with $^1\text{O}_2$ destroying the chromophore and, therefore, the decrease in absorbance at 418 nm can be used as a measure of how much $^1\text{O}_2$ is produced.²⁸ To avoid the background reaction of light with triplet oxygen ($^3\text{O}_2$) producing $^1\text{O}_2$ in an open air atmosphere,²⁹ white light was used at an intensity that decreased the intensity of DPBF (100 mM) absorption at 418 nm by 10% after 30 min (Fig. S3a†). This ensured that

enough light was present to generate $^1\text{O}_2$, but not too much that it would mask $^1\text{O}_2$ generation from the complexes under investigation. The experiment was run in DMSO to ensure that **15** and **16** (both $150 \mu\text{M}$) were fully solubilised. Fig. S3a-c† show that the decrease in absorbance at 418 nm was very similar in either the presence (Fig. S3b and c†) or absence (Fig. S3a†) of the Pt complexes, and the combined normalised results are shown in Fig. 4. Each compound shows a linear degradation of DPBF over time. All three systems and conditions (DPBF alone, DPBF with **15** and DPBF with **16**) gave very similar results. The slope of DPBF alone (-0.0033 min^{-1}) and with **15** (-0.0031 min^{-1}) are almost identical. The slope of DPBF with **16** (-0.0037 min^{-1}) gives a measurably, albeit very slight improvement in $^1\text{O}_2$ generation. From this data, we can conclude that for therapeutic purposes both **15** and **16** should be considered inactive as ROS generators.

Cancer cell viability studies. Finally, to measure the effect of Pt-based systems **15**, **16**, **17** and **35** in the cell viability of cancer cells, preliminary investigations utilising the AlamarBlue® assay were explored using the HL-60 leukaemia cell line (see details in ESI†). These compounds were dissolved in DMSO in a stock solution and tested in cells at a final concentration of 0.1% DMSO in buffer. Since these compounds crystallised out of DMSO/H₂O solutions over a period of months, were stable for at least one year in DMSO-*d*₆ at room temperature (as adjudged by ^1H NMR) and could be heated to $80 \text{ }^\circ\text{C}$ in DMSO-*d*₆ and cooled to room temperature without a noticeable change in the ^1H NMR spectrum, we were confident that DMSO would not interfere with the cell viability experiments over three days at $37 \text{ }^\circ\text{C}$. The calculated IC₅₀ values using 10 000 and 40 000 cells per well are shown in Table 2. Binuclear complex **25** had weak but still measurable cytotoxicity with 10 000 cells per well assays

Table 2 IC₅₀ values calculated for Pt complexes in HL-60 cells using the AlamarBlue® assay

Compd	IC ₅₀ ± SEM ^a (μM) 10 000 cells per well	IC ₅₀ ± SEM ^b (μM) 40 000 cells per well
15	>100	>100
16	55.29 ± 3.0	66.82 ± 5.9
17	100.81 ± 3.4	>100
25	>100	>100
Carboplatin	12.62 ± 1.7	N/A

^a Cells were seeded at a density of 5×10^4 cells per mL in a 96-well plate and treated with the compounds dissolved in 0.1% DMSO in ddH₂O at 10 μM, 25 μM, 50 μM, 75 μM and 100 μM. Carboplatin (dissolved in ddH₂O) was used as a reference and tested in the same manner. Once treated, cells were incubated for 72 h at $37 \text{ }^\circ\text{C}$ after which they were treated with AlamarBlue® and left in darkness in an incubator for 5 h. The resulting fluorescence was read using a plate reader from which percentage viability was calculated. IC₅₀ values were calculated using Prism GraphPad 5 software from at least three independent experiments performed in triplicate. ^b As note (a) but cells were seeded at a density of 2×10^5 cells per mL.



(IC₅₀ = 101 μM); however, this is lost when running the experiments with 40 000 cells per well (IC₅₀ > 100 μM). The cycloplatinated 2-aminoimidazoline complex **16** was the most active (IC₅₀ = 55 μM in 10 000 cells per well and IC₅₀ = 65 μM in 40 000 cells per well) indicating that the five-membered 2-aminoimidazoline ring may be important for activity. Furthermore, the cytotoxicity of Pt complex **16** compares well to the bioactive mono- and bis-isouronium and bis-hydroxyguanidinium families previously tested in our group.³⁰

It is interesting to note that the free ligand in complex **25** (*i.e.* compound **21**) had previously been shown to have no activity in HL-60 cells;³¹ however, complexation with Pt resulted in a weak though measurable effect on cell viability.

Experimental

Synthesis

Preparation of cycloplatinated arylguanidine and 2-arylaminoimidazoline complexes. A suspension of *cis*-[PtCl₂(DMSO)₂] (1.0 eq., 0.888 mmol), the appropriate free base (1.0 eq., 0.888 mmol) in DMSO (1 mL) or in a fresh NaOMe solution (1.1 eq., 1.00 mmol in MeOH, 24 mL) was heated to 80 °C for 2–48 h. MeOH was removed *in vacuo* and the solid was dissolved in a minimum of DMSO (*ca.* 1 mL), filtered through cotton wool and precipitated using H₂O (5–30 mL). The fine solid was collected by centrifugation (8000 rpm), re-dissolved in DMSO (0.2 mL) and precipitated with H₂O if necessary. The powder was dried at rt *in vacuo* overnight at *ca.* 10 mbar.

***α*-Chlorido-*b*-(DMSO-*S*)-*cd*-(2-phenyl)-κC²-guanidine-κN platinum(II) (**15**).** Free base **8** (119 mg, 0.888 mmol) and *cis*-[PtCl₂(DMSO)₂] (360 mg, 0.888 mmol) were added to a freshly prepared NaOMe solution produced from Na metal (24 mg, 1.00 mmol) and MeOH (24 mL), affording after precipitation the title compound as a yellow solid (94 mg, 24%). Crystals suitable for XRD were grown over three months by slow evaporation of H₂O into a concentrated solution of the title compound in DMSO. δ_H (400 MHz, DMSO-*d*₆): 3.35 (s, 6H, CH₃), 6.19 (br s, 1H, PtNH), 6.31 (br s, 2H, NH₂), 6.59–6.72 (m, 2H, Ar-3 & Ar-4), 6.96 (t, 1H, J 7.4, Ar-5), 7.97 (d + dd, 1H, J 7.7 + J 62.6, Ar-6), 9.13 (br s, 1H, ArNH). δ_C (100 MHz, DMSO-*d*₆): 46.2 (CH₃), 113.1 (q Ar-1), 115.0 (CH Ar-3), 121.2 (CH Ar-4), 124.1 (CH Ar-5), 137.0 (q Ar-2), 138.3 (CH Ar-6), 150.4 (q C=N). δ_{Pt} (86 MHz, DMSO-*d*₆): –3582. ν_{max} (ATR)/cm⁻¹: 3407 (NH), 3310 (N), 3193 (NH), 2352, 1645 (C=N), 1602, 1551, 1479, 1399, 1300, 1091 (S–O), 1022, 758, 721. % Calculated for C₉H₁₄N₃OPtClS·0.5NaCl·1.5H₂O·0.5DMSO: C 22.32, H 3.28, N 7.81. % Found: C 22.12, H 3.01, N 8.01. LRMS (*m/z* ESI⁺) found: 444.2 ([M + H]⁺). C₉H₁₅N₃OSCl₂Pt requires 444.03.

***α*-Chlorido-*b*-(DMSO-*S*)-*cd*-[(2-aminophenyl)-κC²-imidazoline-κN]platinum(II) (**16**).** Free base **13** (200 mg, 1.15 mmol) and *cis*-[PtCl₂(DMSO)₂] (462 mg, 1.15 mmol) were added to a freshly prepared NaOMe solution produced from Na metal (29 mg, 1.18 mmol) and MeOH (25 mL), affording after precipitation the title compound as a dark blue solid (90 mg, 18%). M.P. 223–224 °C. Crystals suitable for XRD were grown over three months by slow evaporation of H₂O into a concentrated solution of the title compound in DMSO. δ_H (400 MHz, DMSO-*d*₆): 3.14–3.57 (m, 8H,

2 × CH₃ & CH₂), 3.99 (br s, 2H, CH₂), 6.37–6.77 (m, 2H, Ar-3 & Ar-4), 6.77–7.11 (m, 1H, Ar-5), 7.11–7.57 (m, 1H, NH), 7.57–8.01 (m, 1H, Ar-6), 9.53 (br s, 1H, NH). δ_C (100 MHz, DMSO-*d*₆): 44.0 (CH₂), 46.1 (CH₃), 51.5 (CH₂), 114.9 (q Ar-1), 115.0 (CH Ar-4), 121.8 (CH Ar-3), 124.6 (CH Ar-5), 137.8 (q Ar-2), 139.6 (CH Ar-6), 156.0 (q C=N). δ_{Pt} (86 MHz, DMSO-*d*₆): –3633. ν_{max} (ATR)/cm⁻¹: 3339, 3282 (NH), 3185 (NH), 2994 (CH), 1606, 1578, 1465, 1413, 1288, 1094, 1017, 743. % Calculated for C₁₁H₁₇N₃·OPTClS·H₂O·0.5DMSO: C 27.35, H 3.73, N 7.97. % Found: C 27.16, H 3.45, N 8.16.

Bis-Pt complex of 2-aminophenylguanidine (17**).** Free base **10** (15 mg, 0.1 mmol) and *cis*-[PtCl₂(DMSO)₂] (20 mg, 0.05 mmol) were dissolved in DMSO-*d*₆ (1 mL), affording after precipitation the title compound as a dark purple solid (6 mg, 24%). Crystals suitable for XRD were grown over three months by slow evaporation of H₂O into a concentrated solution of the title compound in DMSO.

Triiodo-tris(4-methoxyguanidine)bis-platinum(III) complex (18**).** To K₂PtCl₄ (41 mg, 0.1 mmol) in H₂O (1 mL) at 60 °C, was added KI (100 mg, 0.6 mmol). The mixture was stirred in the dark for 20 min, after which free base **9** (37 mg, 0.2 mmol) was added. The yellow mixture was stirred at r.t. for 15 min and the brown precipitate was filtered and washed with H₂O. The compound was dissolved in EtOAc and crystallised out by slow evaporation of hexane to give crystals suitable for XRD. No further characterisation data is available for this compound.

***trans*-[Dichloro(DMSO)(2-[phenylamino]imidazoline-κN)platinum] (**19**).** To a solution of K₂PtCl₄ (139 mg, 0.335 mmol) in H₂O (0.5 mL) was added dropwise a solution of DMSO (24 μL, 0.335 mmol) in H₂O (0.5 mL) and the reaction was stirred at r.t. for 4 h until the colour changed from red to yellow. The solid free base **13** (54 mg, 0.335 mmol) and CH₂Cl₂ (0.5 mL) were then added, and the reaction was stirred at r.t. for 16 h. The organic layer was separated and evaporated at r.t. by blowing with Ar to give a crude oil which was purified on silica, eluting in 0.5% acetone in CH₂Cl₂ to give the title compound as a yellow solid (33 mg, 19%). Crystals suitable for XRD were grown over 4 h by slow evaporation of Et₂O into a concentrated solution of the title compound in CH₂Cl₂. δ_H (400 MHz, DMF-*d*₇): 3.37 (s, 6H, CH₃), 3.59 (t, 2H, J 9.1, CH₂), 3.85 (t, 2H, J 9.1, CH₂), 7.15 (br s, 1H, NH), 7.20 (t, 1H, J 7.4, *p*-Ar), 7.30 (d, 2H, J 7.5, *o*-Ar), 7.38–7.43 (m, 2H, *m*-Ar), 8.88 (br s, 1H, NH). δ_C (100 MHz, DMF-*d*₇): 42.5 (CH₃), 43.5 (CH₂), 51.4 (CH₂), 123.1 (CH *o*-Ar), 124.8 (CH *p*-Ar), 129.4 (CH *m*-Ar), 138.6 (q Ar), 160.7 (q C=N). δ_{Pt} (86 MHz, DMF-*d*₇): –3033. ν_{max} (ATR)/cm⁻¹: 3289 (NH), 3090 (NH), 1617 (C=N), 1093 (S–O), 3018, 1588, 1571, 1478, 1432, 1267, 1022, 730. HRMS (*m/z* ESI⁻) Found: 503.0063 ([M – H]⁻). C₁₁H₁₆N₃OSCl₂Pt requires 503.0039.

***cis*-[Dichloro(phenyliminoguanidine (N,N'))platinum] (**20**).** To a crude mixture of **19** prior to column chromatography was added CH₃CN (1 mL). Crystals suitable for XRD were grown over a period of months from this standing solution. δ_H (400 MHz, DMF-*d*₇): 3.52–3.58 (m, 2H, CH₂), 4.25–4.33 (m, 2H, CH₂), 6.55 (br s 1H, NH), 7.75–7.81 (m, 3H, Ar), 7.86–7.90 (m, 2H, Ar), 10.04 (br s, 1H, NH). NOTE: CH₃ obscured by H₂O peak. δ_C (100 MHz, DMF-*d*₇): decomposed over time of experiment (*v* dilute). ν_{max}



(ATR)/cm⁻¹: 3390, 3254 (NH), 2350, 2164 (CN), 1622(C=N), 1576, 1436, 1271, 1098, 1030, 730.

4,4'-Bis-[*a*-chlorido-*b*-(DMSO-*S*)-*cd*-(2-phenyl)-κC²-guanidine-κN]platinum(II)ketone (25). Free base **21** (15 mg, 0.05 mmol) and *cis*-[PtCl₂(DMSO)₂] (40.5 mg, 0.1 mmol) dissolved in DMSO-*d*₆ (1 mL) at 80 °C for 48 h, afforded after precipitation the title compound as a yellow solid (16 mg, 32%). M.p. 250 °C. Crystals suitable for XRD were grown over three months by slow evaporation of H₂O into a concentrated solution of the title compound in DMSO. δ_H (400 MHz, DMSO-*d*₆): 3.36 (s, 12H, CH₃), 6.40 (d, 2H, J 2.5, PtNH), 6.43 (s, 4H, NH₂), 6.75 (d, 2H, J 8.2, Ar-5), 7.38 (dd, 2H, J 1.9, J 8.2, Ar-6), 8.48 (d, 2H, J 1.9, Ar-2), 9.48 (d, 2H, J 2.5, NH). δ_C (150 MHz, DMSO-*d*₆): 46.0 (CH₃), 112.2 (q Ar C-3), 114.4 (Ar C-5), 126.4 (Ar C-6), 131.0 (Ar C-1), 140.3 (q Ar C-4), 140.8 (Ar C-2), 150.1 (q C=N), 194.4 (q C=O). δ_{Pt} (86 MHz, DMSO-*d*₆): -3556, -3559. ν_{max} (ATR)/cm⁻¹: 3356 (NH), 3206 (NH), 3000, 2917 (CH), 1649, 1619, 1535, 1477, 1304, 1288, 1249, 1093, 1017, 1002, 947, 823, 748, 677. % Calculated for C₁₉H₂₆N₆O₃Pt₂Cl₂S₂·6NaCl·6H₂O·4DMSO: C 19.27, H 2.55, N 4.99. % Found: C 19.32, H 2.90, N 5.21.

ROS generation experimental details

For the evaluation of the singlet oxygen production, solutions the ¹O₂ trap 1,3-diphenylisobenzofuran (DPBF) in DMSO were employed (20 mg in 50 mL). Calibration was achieved using 50 : 50 of a 112 μM DPBF solution to get absorption 1 at λ_{max} = 418 nm (in DMSO). Next, a fresh solution of each Pt complex (**15**, or **16**) in DMSO was prepared at high concentration (150 μM), added to the cuvette and its absorbance was adjusted to around 0.01 at wavelength of irradiation. Potential singlet oxygen production was assessed looking at the decay absorption spectra of DPBF at time points 0, 2, 5, 10, 20, and 30 min. Since no clear effect was observed in the presence of the DMSO Pt(II) complexes solutions, no further measurements at a lower concentrations were carried out. The slope of plots of absorbance of DPBF at 418 nm vs. irradiation time for each photosensitizer was calculated.

Cell viability experimental details

The HL-60 (human caucasian promyelocytic leukemia) cell line was maintained between 200 000–2 000 000 cells per mL in Roswell Park Memorial Institute (RPMI) 1640 medium with stable glutamate (GlutaMax I) supplemented with 10% (v/v) foetal bovine serum (FBS) and 50 μg per mL penicillin/streptomycin (pen-strep). The growth medium was stored in the fridge at 4 °C and heated to 37 °C prior to culture work. Cells were grown at 37 °C in a humidified environment maintained at 95% O₂ and 5% CO₂ and passaged at least three times weekly depending on their levels of confluency. When required for sub-culturing, cells were transferred to a sterile tube and centrifuged at 1296 rpm for 5 min. The supernatant was discarded, and the cell pellet was resuspended in fresh medium. Cells were then counted using a haemocytometer slide and seeded at the required density.

HL-60 cells in the log phase of growth were seeded in 96-well plates at a density of 50 000 cells per mL (200 μL per well or 10

000 cells per well) in complete RPMI medium the same day of the experiment. Compounds **13**, **16**, **17** and **25** were dissolved in DMSO to obtain a starting 100 mM stock solution. The cells were then treated with either 2 μL of a 1 : 100 dilution of stock concentrations of drugs or ddH₂O as vehicle control, or 0.2 μL of a 1 : 1000 dilution of stock concentrations of drugs or DMSO as vehicle control. All experiment were repeated in triplicate for at least three times. Three wells containing 200 μL RPMI with no cells were also set up as blanks.

After 72 h incubation, 20 μL AlamarBlue® was added to each well. The plates were incubated in darkness at 37 °C for 5 hours. Using a Molecular Devices microplate reader, the fluorescence (*F*) was then read at an excitation wavelength of 544 nm and an emission wavelength of 590 nm. Cell viability was then determined by subtracting the mean blank fluorescence (*F*_b) from the treated sample fluorescence (*F*_s) and expressing this as a percentage of the fluorescence of the blanked vehicle control (*F*_c). This is demonstrated in the equation below. The results were then plotted as nonlinear regression, sigmoidal dose-response curves on Prism GraphPad 5 software, from which the IC₅₀ value for each drug was determined.

$$\frac{(F_s - F_b)}{(F_c - F_b)} \times \frac{100}{1} = \% \text{ cell viability}$$

Conclusions

The preparation of Pt(II) complexes of aryl guanidines has been explored. Suitable conditions have been found for the preparation of unsubstituted phenyl guanidine-like Pt(II) cyclometallated complexes. However, replacement of the phenyl system by a pyridine, separation of the guanidine and phenyl moieties by a methylene group or *p*-substitution of the phenyl ring with -OCH₃ did not result in the corresponding cyclometallated complexes. Only *o*-substitution of the phenyl ring with a NH₂ provided a bimetallic Pt(II) complex (**17**) combining cyclometallation and coordination with each of the Pt centres. Additionally, an *in situ* activation of Pt-arylguanidine complexes with acetonitrile to create a bidentate aryl iminoguanidine Pt(II) complex are reported. The cyclometallation methodology was extended to create a water-stable conjugate incorporating two Pt(II) ions and a diaryl bis-guanidine DNA minor groove binder previously reported by us. The cyclometallated Pt(II) complexes were particularly stable to aqueous environments and some of them were tested for ROS generation and anticancer activity in HL-60 cells.

Data availability

The following ESI† is available: high temperature ¹H NMR experiments for the formation of complex **15**; preparation of mono-guanidinium-like derivatives used as precursors of the ligands used to explore Pt complexation conditions (*i.e.* aryl guanidinium salts **1–7** and the corresponding precursors bis-Boc-protected guanidines **S6**, **S7–S8**, **S9–S10**, **S13–S14**); experimental details of the methods utilised; reaction of compound



21 with *cis*-[PtCl₂(DMSO)₂] followed by ¹H NMR; graphs showing the experiments with complexes 15 and 16 searching for ROS generation; biochemical details (*i.e.* cell viability assays); X-ray crystallographic data for compounds 15, 16, 17, 18, 19, 20, and 25.

Author contributions

Conceptualization, I. R. and C. J. M.; methodology, I. R., C. J. M. and A. R. McD.; data analysis, P. O'. S., V. P., B. T., C. J. M., A. R. McD., and I. R.; experiments, P. O'. S., V. P., and B. T.; writing and editing, P. O'. S., V. P., B. T., C. J. M., A. R. McD., and I. R.; supervision, I. R., C. J. M. and A. R. McD. All authors have read and agreed to the published version of the manuscript.

Conflicts of interest

There are no conflicts to declare.

Acknowledgements

This work has been funded by Science Foundation Ireland (SFI-RFP project: CH3060). P. O'. S. thanks SFI (SFI-RFP, project: CH3060) and V. P. thanks the School of Chemistry at Trinity College Dublin for postgraduate funding. We thank Dr John O'Brien for expert NMR studies and Dr Aaron Keogh for preliminary work in Pt-guanidine complexation. We also would like to thank Carsten Lenczyk, Bruker AXS for his insight and assistance.

References

- 1 S. Rottenberg, C. Disler and P. Perego, The rediscovery of platinum-based cancer therapy, *Nat. Rev. Cancer*, 2021, **21**(1), 37–50.
- 2 T. C. Johnstone, K. Suntharalingam and S. J. Lippard, The Next Generation of Platinum Drugs: Targeted Pt(II) Agents, Nanoparticle Delivery, and Pt(IV) Prodrugs, *Chem. Rev.*, 2016, **116**(5), 3436–3486.
- 3 T. Zhong, J. Yu, Y. Pan, N. Zhang, Y. Qi and Y. Huang, Recent Advances of Platinum-Based Anticancer Complexes in Combinational Multimodal Therapy, *Adv. Healthcare Mater.*, 2023, **12**(22), e2300253.
- 4 S. Alassadi, M. J. Pisani and N. J. Wheate, A chemical perspective on the clinical use of platinum-based anticancer drugs, *Dalton Trans.*, 2022, **51**(29), 10835–10846.
- 5 *Drug Monitoring and Clinical Chemistry*, ed. Hempel G., Universität Münster, Germany: Institut für Pharmazeutische und Medizinische Chemie, 2004, Chapter 7: Hempel G, Dose and therapy individualisation in cancer chemotherapy.
- 6 (a) T. C. Johnstone, K. Suntharalingam and S. J. Lippard, The Next Generation of Platinum Drugs: Targeted Pt(II) Agents, Nanoparticle Delivery, and Pt(IV), *Prodrugs Chem Rev.*, 2016, **116**(5), 3436–3486; (b) T. C. Johnstone, J. J. Wilson and S. J. Lippard, Monofunctional and Higher-Valent Platinum Anticancer Agents, *Inorg. Chem.*, 2013, **52**(21), 12234–12249.
- 7 (a) R. G. Kenny and C. J. Marmion, Toward Multi-Targeted Platinum and Ruthenium Drugs- A New Paradigm in Cancer Drug Treatment Regimens?, *Chem. Rev.*, 2019, **119**, 1058–1137; (b) R. G. Kenny, S. W. Chuah, A. Crawford and C. J. Marmion, Platinum(IV) Prodrugs – A Step Closer to Ehrlich's Vision?, *Eur. J. Inorg. Chem.*, 2017, **2017**(12), 1596–1612; (c) A. Khoury, K. M. Deo and J. R. Aldrich-Wright, Recent advances in platinum-based chemotherapeutics that exhibit inhibitory and targeted mechanisms of action, *J. Inorg. Biochem.*, 2020, **207**, 111070.
- 8 A. R. Gomes, C. L. Varela, A. S. Pires, E. J. Tavares-da-Silva and M. F. Roleira, Synthetic and natural guanidine derivatives as antitumor and antimicrobial agents: a review, *Bioorg. Chem.*, 2023, **138**, 106600.
- 9 P. J. Bailey and S. Pace, The coordination chemistry of guanidines and guanidates, *Coord. Chem. Rev.*, 2001, **214**, 91–141.
- 10 A. A. Legin, M. A. Jakupec, N. A. Bokach, M. R. Tyan, V. Y. Kukushkin and B. K. Keppler, Guanidine platinum(II) complexes: synthesis, *in vitro* antitumor activity, and DNA interactions, *J. Inorg. Biochem.*, 2014, **133**, 33–39.
- 11 F. Carrillo-Hermosilla, R. Fernández-Galán, A. Ramos and D. Elorriaga, Guanidates as Alternative Ligands for Organometallic Complexes, *Molecules*, 2022, **27**, 5962.
- 12 P. Elumalai, N. Thirupathi and M. Nethaji, Dual Role of Acetate as a Nucleophile and as an Internal Base in Cycloplatination Reaction of sym N,N',N''-Triarylguanidines, *Inorg. Chem.*, 2013, **52**(4), 1883–1894.
- 13 D. Nieto, S. Bruña, A. M. González-Vadillo, J. Perles, F. Carrillo-Hermosilla, A. Antiñolo, J. M. Padrón, G. B. Plata and I. Cuadrado, Catalytically generated ferrocene-containing Guanidines as efficient precursors for new redox-active heterometallic Platinum(II) complexes with anticancer activity, *Organometallics*, 2015, **34**, 5407–5417.
- 14 M. Marin-Luna, G. Sanchez-Sanz, P. O'Sullivan and I. Rozas, Guanidine Complexes of Platinum: A Theoretical Study, *J. Phys. Chem. A*, 2014, **118**(29), 5540–5547.
- 15 D. Aitken, A. Albinati, A. Gautier, H. P. Husson, G. Morgant, D. Nguyen-Huy, J. Kozelka, P. Lemoine, S. Ongeri, S. Rizzato and B. Voissat, Platinum(II) and Palladium(II) complexes with *N*-aminoguanidine, *Eur. J. Inorg. Chem.*, 2007, **2007**(21), 3327–3334.
- 16 T. Yamada, X. Liu, U. Englert, H. Yamane and R. Dronskowski, Solid-state structure of free base guanidine achieved at last, *Chem.-Eur J.*, 2009, **15**(23), 5651–5655.
- 17 U. Wild, P. Roquette, E. Kaifer, J. Mautz, O. Hübner, H. Wadepohl and H. J. Himmel, Synthesis and Structural Characterisation of *cis*- and *trans*-[(hpp H)₂PtCl₂], [(hpp H)₃PtCl] + Cl⁻ and Some new Salts of the [hpp H₂]⁺ Cation (hpp H = 1,3,4,6,7,8-Hexahydro-2H-pyrimido [1,2-*a*]pyrimidine): the Importance of Hydrogen Bonding, *Eur. J. Inorg. Chem.*, 2008, **8**, 1248–1257.



- 18 P. Elumalai, N. Thirupathi and M. Nethaji, Dual role of acetate as a nucleophile and as an internal base in cycloplatination reaction of *sym-N,N',N''*-triarylguanidines, *Inorg. Chem.*, 2013, **52**(4), 1883–1894.
- 19 J. H. Price, A. N. Williamson, R. F. Schramm and B. B. Wayland, Palladium(II) and platinum(II) alkyl sulfoxide complexes. Examples of sulfur-bonded, mixed sulfur- and oxygen-bonded, and totally oxygen-bonded complexes, *Inorg. Chem.*, 1972, **11**(6), 1280–1284.
- 20 D. Griffith, M. P. Morgan and C. J. Marmion, A novel anti-cancer bifunctional platinum drug candidate with dual DNA binding and histone deacetylase inhibitory activity, *Chem. Commun.*, 2009, **2009**(44), 6735–6737.
- 21 V. Sicilia, M. Baya, P. Borja and A. Martín, Oxidation of half-lantern Pt(II,II) compounds by halocarbons. Evidence of dioxygen insertion into a Pt(III)-CH₃ bond, *Inorg. Chem.*, 2015, **54**(15), 7316–7324.
- 22 E. Anger, M. Rudolph, C. Shen, N. Vanthuyne, L. Toupet, C. Roussel, J. Autschbach, J. Crassous and R. Réau, From hetero- to homochiral bis(metallahelicene)s based on Pt(III)-Pt(III) bonded scaffold: isomerization, structure, and chiroptical properties, *J. Am. Chem. Soc.*, 2011, **133**(11), 3800–3803.
- 23 K. Matsumoto and M. Ochiai, Organometallic chemistry of platinum-blue derived platinum III dinuclear complexes, *Coord. Chem. Rev.*, 2002, **231**(1–2), 229–238.
- 24 S. U. Pandya, K. C. Moss, M. R. Bryce, A. S. Batsanov, M. A. Fox, V. Jankus, H. A. Al Attar and A. P. Monkman, Luminescent platinum (II) complexes containing cyclometallated diaryl ketimine ligands: synthesis, photophysical and computational properties, *Eur. J. Inorg. Chem.*, 2010, **2010**(13), 1963–1972.
- 25 Y. Y. Scaffidi-Domianello, A. A. Nazarov, M. Haukka, M. Galanski, B. K. Keppler, J. Schneider, P. Du, R. Eisenberg and V. Y. Kukushkin, First example of the solid-state thermal cyclometallation of ligated benzophenone imine giving novel luminescent platinum(II) species, *Inorg. Chem.*, 2007, **46**(11), 4469–4482.
- 26 V. Y. Kukushkin and A. J. L. Pombeiro, Additions to metal-activated organonitriles, *Chem. Rev.*, 2002, **102**(5), 1771–1802.
- 27 D. Ashen-Garry and M. Selke, Singlet Oxygen Generation by cyclometalated complexes and applications, *Photochem. Photobiol.*, 2014, **90**(2), 257–274.
- 28 W. Spiller, H. Kliesch, D. Wöhrle, S. Hackbarth, B. Röder and G. Schnurpfeil, Singlet oxygen quantum yields of different photosensitizers in polar solvents and micellar solutions, *J. Porphyrins Phthalocyanines*, 1998, **2**(2), 145–158.
- 29 P. R. Ogilby, Singlet oxygen: there is indeed something new under the sun, *Chem. Soc. Rev.*, 2010, **39**, 3181–3209.
- 30 A. Kahvedžić, S. M. Nathwani, D. M. Zisterer and I. Rozas, Aromatic bis-N-hydroxyguanidinium derivatives: synthesis, biophysical and biochemical evaluations, *J. Med. Chem.*, 2013, **56**(2), 451–459.
- 31 A. Kahvedžić, PhD thesis, University of Dublin, 2011.

